



# EXPLORING MULTIFRACTALITY IN MOTOR IMAGERY

A LONGITUDINAL COMPARISON OF LINEAR AND  
NON-LINEAR METRICS IN BRAIN-COMPUTER  
INTERFACES

JOS PRINSEN

THESIS SUBMITTED IN PARTIAL FULFILLMENT  
OF THE REQUIREMENTS FOR THE DEGREE OF  
MASTER OF SCIENCE IN COGNITIVE SCIENCE & ARTIFICIAL INTELLIGENCE

DEPARTMENT OF  
COGNITIVE SCIENCE & ARTIFICIAL INTELLIGENCE  
SCHOOL OF HUMANITIES AND DIGITAL SCIENCES  
TILBURG UNIVERSITY

**STUDENT NUMBER**

2040874

**COMMITTEE**

dr. Travis Wiltshire  
dr. Paris Mavromoustakos Blom

**LOCATION**

Tilburg University  
School of Humanities and Digital Sciences  
Department of Cognitive Science &  
Artificial Intelligence  
Tilburg, The Netherlands

**DATE**

June 24, 2024

**WORD COUNT**

8820

# EXPLORING MULTIFRACTALITY IN MOTOR IMAGERY

A LONGITUDINAL COMPARISON OF LINEAR AND  
NON-LINEAR METRICS IN BRAIN-COMPUTER INTERFACES

JOS PRINSEN

## Abstract

Brain-computer interfaces (BCI) hold the promise of revolutionizing human-computer interaction by translating mental processes into commands for external devices, with Motor Imagery (MI) where an individual imagines performing a motor action. MI-based BCIs face challenges due to user variability and inconsistent brain activity patterns. This thesis explores the potential of Multifractal Detrended Fluctuation Analysis (MFDFA), a non-linear analysis method, to better understand the complex brain dynamics during MI, aiming to improve BCI performance. Analyzing electroencephalogram (EEG) data from 62 participants engaged in MI tasks over multiple sessions, the study compares traditional linear features with non-linear multifractal features to uncover how these metrics behave during MI and evolve with training. Key findings indicate that MI phases exhibit higher multifractal complexity than rest, with successful trials showing distinct multifractal behaviors. High-performing participants demonstrate significant contralateralization in both linear and non-linear metrics, unlike low performers. Temporal analysis reveals that multifractal complexity increases with MI training, suggesting enhanced neural efficiency and specificity. These insights could enhance BCI systems' reliability and effectiveness, particularly for users with severe motor impairments, by providing more robust metrics for classification, thereby improving BCI accessibility and performance across diverse user groups.

## 1 DATA SOURCE, ETHICS, CODE, AND TECHNOLOGY STATEMENT

The data used in this thesis was made open source in parallel to the following paper: Mindfulness Improves Brain-Computer Interface Performance by Increasing Control Over Neural Activity in the Alpha Band [Stieger et al. \(2020\)](#). The thesis did not involve any data collection. The owner of the data made it publicly available, and gave consent for using it in further publication. The data was acquired through Figshare: Human

EEG Dataset for Brain-Computer Interface and Meditation. All figures and images were created specifically for this project. No code from other papers was utilized, however, some parts of the ERD calculation were based on a paper by citeMa2020 . All packages and package versions are listed in the coding environment provided with the thesis on Github: <https://github.com/JosPrinsen/MasterThesis.git>. ChatGPT was used for generating both Python and R code for the analysis, as well as for rephrasing texts to improve academic language use. Zotero was employed for reference management.

## 2 INTRODUCTION

Imagine a technology that not only responds to our commands but understands our intentions. Brain-computer interfaces (BCIs) promise such an interface, with Motor Imagery (MI) serving as a cornerstone for these revolutionary systems (Padfield, Zabalza, Zhao, Masero, & Ren, 2019). MI is a mental process that can be captured through electroencephogram (EEG), where an individual envisions performing a motor action without physically executing it, allowing for control of external devices through a BCI. Yet, despite significant advancements, MI BCIs frequently face inefficiencies due to user variability, classification system limitations, and inconsistent brain activity patterns across trials and sessions (Zhang, Li, Zhang, Yao, & Xu, 2020). These inefficiencies are detrimental for such BCIs as they can make the system unusable for a small group of users who cannot consistently generate the correct brain activity patterns, and changes over time can reduce the system's reliability, introducing the need for constant recalibration to maintain accuracy and effectiveness. Traditional linear analysis methods, while foundational, might not capture all components of the brain's intricate communication patterns (Aftanas & Golocheikine, 2002). To address these challenges, more sophisticated analysis methods are needed.

This thesis proposes to explore a non-linear analysis method, namely Multifractal Detrended Fluctuation Analysis (MFDFA), to delve deeper into the brain related dynamics that occur during MI. MFDFA is a statistical method used to analyze scale-invariant properties and multifractality in non-stationary time series data (Kelty-Stephen, Lane, Bloomfield, & Mangalam, 2022; Kelty-Stephen, Palatinus, Saltzman, & Dixon, 2013). In other words, MFDFA is a method used to detect and measure varying patterns in small and large time scales/fragments over different statistical moments (Kelty-Stephen et al., 2013). MFDFA is ideal for investigating EEG data, which captures electrical activity in the brain during MI, due to its ability

to reveal complex, scale-invariant patterns and multifractal characteristics inherent in neural signals [Chatterjee, Pratiher, and Bose \(2017\)](#).

In the past, Multifractal analysis has been used to analyze EEG signals with different goals, such as detecting epileptic zones in EEG ([Sikdar, Roy, & Mahadevappa, 2018](#)), classifying emotional states ([Paul, Mazumder, Ghosh, Tibarewala, & Vimalarani, 2015](#)), or differentiate between cognitive states, such as motor, perception, and attention tasks, achieving notable classification accuracy ([Gaurav, Anand, & Kumar, 2021](#)). Despite these successes, there are no studies specifically examining or interpreting multifractal behavior in MI. The main goal of this thesis is to understand how these nonlinear metrics behave during MI by contrasting them to the traditional linear metrics, which could lead to enhanced BCI's in the future.

This study investigates the brain activity of participants as they train to imagine left or right directional movements over multiple trials and sessions. Performance is measured by the accuracy of classified EEG signal patterns corresponding to the intended movements ([Stieger et al., 2020](#)). By comparing traditional linear features with nonlinear multifractal features of MI, and examining their changes over time, the study aims to uncover novel insights into the role of multifractal descriptors in MI. This analysis could potentially reveal how individual differences in learning speed and MI improvement are reflected in non-linear EEG properties, shedding light on the cognitive and neural mechanisms of MI-BCI training. Additionally, since no studies have examined the evolution of multifractal metrics in brain activity over a longitudinal scale, this research could offer insights into the complex long-term processes of neural dynamics.

To guide this exploratory analysis, this thesis seeks to address several key research questions that aim to deepen our understanding of the multifractal characteristics of EEG signals during MI. Specifically, this research will investigate the following:

**RQ1** *What are the Multifractal characteristics of EEG signals during motor imagery?*

**RQ2** *Are MFDFA metrics different based on the performance of participants during MI?*

**RQ3** *How do the Multifractal properties of EEG signals evolve with motor imagery training, and how does this compare to traditional linear descriptors?*

These questions are exploratory in nature, and focus on contrasting the complex, non-linear dynamics of brain activity associated with MI with those extracted through traditional linear methods. Ultimately, the findings of this paper might contribute to a greater understanding of the dynamics during MI, which in turn could improve BCI's.

Advancing the understanding and efficiency of BCIs holds significant societal importance. Enhanced BCIs can provide improved communication tools, increased independence, and a higher quality of life for individuals with severe motor impairments. For example, effective BCIs could enable people with disabilities to control prosthetic limbs, operate wheelchairs, or communicate through digital interfaces, all through the power of thought (Tariq, Trivailo, & Simic, 2018). Addressing the inefficiencies in current BCI systems is crucial for making these technologies more reliable and accessible. Additionally, improved BCI technology can reduce healthcare costs and the burden on caregivers by promoting self-sufficiency among users (Geronimo & Simmons, 2020). Ultimately, the findings of this research could be a stepping stone to drive technological progress, where advanced BCI technology is accessible to all who need it.

### 3 RELATED WORK

#### 3.1 *Introduction to Motor Imagery*

MI entails mentally rehearsing a motor action without physical execution (Padfield et al., 2019). This cognitive simulation leverages neural pathways akin to those involved in actual movement (Sheahan, Ingram, Žalalytė, & Wolpert, 2018). BCI systems are capable of classifying the intent from the brain activity generated from this mental simulation, which presents a viable alternative for individuals with mobility impairments or limb loss, such as those affected by paralysis or stroke (Padfield et al., 2019). By envisioning movements, users can interface with prosthetic devices or engage in neurorehabilitation exercises, fostering improvement in motor control through repeated mental practice (Bovend'Eerdt, Dawes, Sackley, Izadi, & Wade, 2010). In neurorehabilitation patients practice MI and enhance their ability to vividly imagine and simulate motor actions without actual movement, which in turn also positively impacts control over physical motor actions (Padfield et al., 2019). Given these promising applications, MI has been extensively studied using techniques such as electroencephalography (EEG), providing a non-invasive means to capture the brain's electrical activity with high temporal resolution, making it suitable for studying dynamic changes in brain activity associated with MI tasks (Lotze & Halsband, 2006; Padfield et al., 2019)

#### 3.2 *Event-related Desynchronization/Synchronization*

Previous research has demonstrated a modulation of oscillatory activity during MI tasks through triggering event-related neural potentials (ERP's)

particularly in the mu (8-13 Hz) and beta (13-30 Hz) frequency bands over sensorimotor regions (SMRs) of the brain (Pfurtscheller, 2000). This modulation, known as event-related desynchronization (ERD) followed by an event-related synchronization (ERS) signifies a decrease in power, followed by an increase in power within the mu and beta frequency bands over the sensorimotor areas, corresponding to an increase in neuronal activity related to the imagined or anticipated motor act (Neuper, Wörz, & Pfurtscheller, 2006; Pfurtscheller, 2000; Pfurtscheller & Da Silva, 1999). The magnitude of ERD/ERS, quantified by the decrease followed by an increase in power, in the mu and beta bands correlates with the degree of engagement of the SMRs (Nakayashiki, Saeki, Takata, Hayashi, & Kondo, 2014; Pfurtscheller & Da Silva, 1999). Studies have shown that as individuals practice motor imagery tasks, the SMRs are more engaged, which is evident from an increase in the magnitude of the ERD (Nakayashiki et al., 2014; Prasad, Herman, Coyle, McDonough, & Crosbie, 2010). While the strength of the ERD changes when improving on MI tasks, the mechanics of such ERD patterns are not consistent between participants, and even over trials within participants (Huang et al., 2023; Wriessnegger, Müller-Putz, Brunner, & Sburlea, 2020). For example, contralateralization may vary, with some participants showing more pronounced bilateral or ipsilateral ERD patterns, especially during complex or less familiar tasks (Lee, Lee, Kim, & Kim, 2020).

### 3.3 *Lateralization in Motor Imagery*

Lateralization in the context of motor imagery refers to the asymmetric activation of brain hemispheres, particularly evident in EEG patterns (Lee et al., 2020). Lateralization, as described by the lateralization index (LI), refers to the difference in power between the hemispheres, indicating the degree of engagement of sensorimotor regions during motor imagery tasks (Nam, Jeon, Kim, Lee, & Park, 2011). High LI values suggest stronger engagement of the contralateral hemisphere, which is critical for the accuracy and performance of MI-BCI systems, whereas negative LI values suggest that ipsilateral is dominating the interaction (Lee et al., 2020; Nam et al., 2011). Studies have shown that the ERD is significantly larger in the hemisphere contralateral to the movement (Doyle, Yarrow, & Brown, 2005). This contralateral dominance is essential for motor selection processes, allowing early preparation and shorter reaction times in tasks where the laterality of the movement is predictable (Doyle et al., 2005; Pfurtscheller & Da Silva, 1999). The pattern of lateralization, however, is not consistent across all individuals, reflecting differences in neural architectures and learning strategies (Huang et al., 2023). Some participants may show more

pronounced bilateral or ipsilateral ERD patterns, especially during complex or less familiar tasks (Huang et al., 2023; Wriessnegger et al., 2020).

### 3.4 *Variability in MI descriptors*

The variability observed between subjects has been attributed to factors such as age, gender, and living habits, which influence the brain's topography and electrophysiological properties, and has been named the BCI inefficiency problem (Huang et al., 2023; Zhang et al., 2020). This diversity in neural architecture and functional organization means that a BCI model trained on one individual often performs poorly when applied to another (Huang et al., 2023). Next to inter subject variability, there is also intra subject variability, where the ERD, and lateralization is different between trials, and session within the same participant (Huang et al., 2023; Zhang et al., 2020). It is believed that intra subject variability arises from fluctuations in psychological and physiological states, such as levels of fatigue, relaxation, concentration, and task familiarity (Huang et al., 2023; Perquin, Van Vugt, Hedge, & Bompas, 2023). These changes can significantly impact the consistency of EEG recordings over time, leading to a decline in BCI performance even within the same individual. The presence of both inter- and intra-subject variability undermines the assumption of independent and identically distributed data sets, which is a cornerstone of conventional machine learning frameworks that are used for classifying MI interactions (Huang et al., 2023).

### 3.5 *Addressing BCI inefficiency*

While some researchers try to address this inter and intra subject variability through means of adaptive classification, for example, through transfer learning, others are exploring new features to use in the classification of MI (Brodu, Lotte, & Lécuyer, 2012). For a comprehensive review of traditional features that are employed for MI, please refer to (Bashashati, Fatourechi, Ward, & Birch, 2007). More recently however, the use of non-linear features has been suggested. According to Kelty-Stephen et al. (2013), it is possible that traditional linear analyses do not fully capture the complexity of physiological data, including EEG activity, as they often assume homogeneity in the data. Non-linear analyses such as multifractal analysis might be able to account for this, as these metrics are designed to capture the intricacies of data that exhibit variability across multiple scales (Ihlen & Vereijken, 2010; Kelty-Stephen et al., 2022).

### 3.6 Multifractal Detrended Fluctuation Analysis

An example of such a multifractal analysis is MultiFractal Detrended Fluctuation Analysis (MFDFA), which is a statistical tool used to explore the complex and self-similar properties of time series data across different scales (Ihlen & Vereijken, 2010; Kelty-Stephen et al., 2022). At its core, MFDFA explores how the statistical moments (e.g., variance or the mean) of signals change as one zooms in or out across different time scales, which in turn reveals the degree of interactivity between time scales (Kelty-Stephen et al., 2013). In terms of brain activity, this interactivity could be interpreted as different neuronal substructures or populations interacting or communicating over multiple spatiotemporal scales, causing emergent behavior visible as brain networks or global activity (Ihlen & Vereijken, 2010).

MFDFA plots yield several important measures for understanding the complexity and variability of time series data. The Hurst exponent ( $H(q)$ ) reveals the degree of long-range dependence across different scales, indicating persistence or anti-persistence in the data. The multifractal spectrum ( $D(h)$ ) illustrates the distribution of singularities, with a wider spectrum indicating greater multifractal complexity and variability in scaling behaviors. Singularity strength ( $h$ ) and its range ( $h_{\max} - h_{\min}$ ) highlight the intensity and diversity of irregularities within the signal. These measures together help in comprehensively understanding the underlying dynamics of the data. For more details on MFDFA, refer to Kelty-Stephen et al. (2013) and Kantelhardt et al. (2002).

MFDFA has widely been used in a variety of different research fields, such as geography, economics and for physiological measures (Gu & Zhou, 2006). MFDFA has also been used to analyze EEG signals. For example, in a study by Gaurav et al. (2021), MFDFA metrics extracted from EEG were used to classify between 6 levels of cognitive states associated with motor, perception, and attention tasks. The study utilized  $H(q)$  values calculated from EEG segments of 10 seconds, reaching an accuracy of around 91%, demonstrating that Hurst exponents can be used to differentiate between tasks which are expected to generate varying levels of complexity in the brain. Moreover, MFDFA features were used for classifying emotions from EEG activity, achieving an average classification accuracy of 84.5% for positive emotions and 82.5% for negative emotions (Paul et al., 2015).

MFDFA measures aren't the only type of non-linear algorithms that capture multifractal dynamics. While MFDFA metrics and multifractal cumulants both aim to capture the multifractal structure and complexity of a timeseries, they do so by slightly different means. MFDFA metrics analyze the scaling behavior of fluctuations, whereas multifractal cumulants

quantify the statistical moments of multifractal measures (Wendt, Abry, & Jaffard, 2007). Interestingly, multifractal cumulants were used to classify MI. Brodu et al. (2012) demonstrates over 13 datasets that multifractal cumulants can be used for classification of left/right hand MI with an average accuracy over all datasets of 75.8%. Moreover, combining these multifractal features with band powers increased the classification accuracy for nearly all datasets to an average of 80.3%. This shows that multifractal features can be used to capture the dynamics needed for MI classification.

Despite the successful application of multifractal features in MI classification, there is a noticeable gap in the understanding of the multifractal behaviour relating to MI dynamics. While both multifractal cumulants and MFDFA features have been successfully used in classifiers for different cognitive tasks, this was always done without any literature explaining how or why the features could help in improving classification accuracy. Instead of incorporating multifractal values directly into a classifier, this thesis aims to take a step back, and try to understand the multifractal dynamics that occur during MI. By analyzing the Hurst exponent, multifractal spectrum, and scaling exponents, the main goal is to uncover the underlying complexities and interactions within MI-related EEG signals, with as ultimate goal to both understand the brain better, but also to increase understanding of the multifractal features that can be used in MI classification.

### 3.7 Temporal analysis of (non)linear metrics

Considering that MI is suffering from inter-trial, and session variability, it is crucial to not investigate one session in isolation, but to investigate these metrics through a temporal scope. Techniques such as the autocorrelation function (ACF) and detrended fluctuation analysis (DFA) can provide additional layers of understanding specifically in the temporal domain (Perquin et al., 2023). These methods have been utilized effectively to analyze temporal dependencies and reveal patterns between trials during sessions of reaction time series, as demonstrated in the study by Perquin et al. (2023) on sensorimotor variability. Autocorrelation helps in quantifying the correlation of a time series with itself over various delays, which can expose the persistence of dependencies across multiple trials (Xu, De Barbaro, Abney, & Cox, 2020). DFA, on the other hand, can assess the scaling properties of the data, highlighting long-range correlations that are not immediately apparent through simple statistical measures (Hardstone et al., 2012).

By comparing how traditional and multifractal measures evolve across multiple sessions, it might be possible to gain new insights into the reasons for BCI inefficiency, as well as, provide possible new features to combat

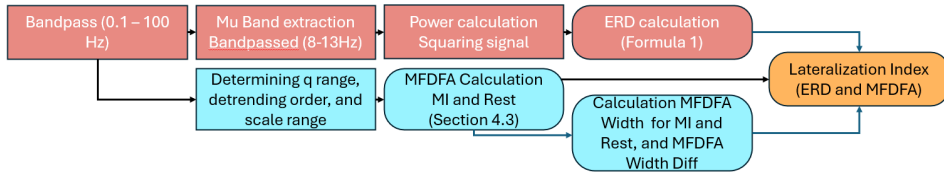


Figure 1: General overview of preprocessing pipeline.

this. Notably, no studies to date have performed a longitudinal analysis of MFDFA values in EEG metrics, let alone for Motor Imagery. This novel approach aims to reveal how multifractal dynamics change over time, potentially identifying specific multifractal characteristics that correlate with MI practice. It would be especially interesting to compare these multifractal metrics to the standard linear metrics for MI to understand their relative effectiveness and potential complementary insights.

#### 4 METHOD

The following section is dedicated to describing the methods and dataset used to perform a longitudinal study of multifractal dynamics for MI. A link to a notebook detailing all analysis steps used during the project can be found in [Prinsen \(2024\)](#). Moreover, a general overview of the steps can be found in Figure 1 and 3

##### 4.1 Dataset Description

The dataset was comprised of de-identified electroencephalogram data from 62 healthy participants, collected during a BCI Motor Imagery study that explored the impact of mind-body awareness training on BCI performance ([Stieger et al., 2020](#)). Participants underwent 7 to 11 BCI training sessions (see [Stieger et al. \(2020\)](#) for list of participants), each aimed at enhancing their ability to control a computer cursor through intended directional thoughts in both one-dimensional (1D) and two-dimensional (2D) tasks. For this study a subset was taken, where only 1D tasks were considered. The directional thoughts were either Left or Right (L/R) imagined cursor movement.

EEG signals were recorded during the Motor Imagery sessions using a 64-electrode setup, with 62 electrodes included in the final dataset. For this study two electrodes were considered, namely C<sub>3</sub> and C<sub>4</sub> [2](#). These channels are above the SMRs, and are chosen due to their known relevance in motor control and motor planning. Data were collected at a sampling rate of 1000 Hz. Each session comprised approximately 450 trials, including both 1D

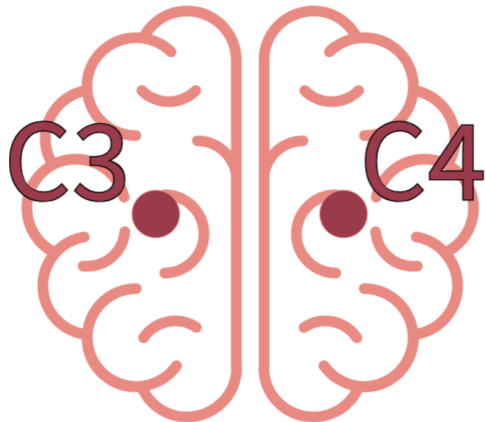


Figure 2: Illustration indicating electrode locations

and 2D tasks, but only the 225 1D trials per session were used for this study. Each trial consisted of a 2-second rest phase, a 2-second presentation phase where the left or right side was highlighted, and an MI phase where participants moved a circle to the left or right side of the screen based on their imagined intent for the circle. Feedback was provided during MI training, by moving the circle according to the classification results of an Autoregressive algorithm, as described in [Stieger et al. \(2020\)](#).

The duration of the MI phase varied based on the participant's speed in completing the task, which ended when the circle reached the left or right side of the screen. Completion was recorded as successful or unsuccessful based on whether the circle reached the correct side. If the MI phase exceeded 6 seconds, the outcome of the trial was based on the circle's position at timeout. For example, if the circle was near the correct side, the forced result was marked as successful; otherwise, it was unsuccessful. Performance for each session was calculated as the number of successful trials divided by the total number of trials. A total of 867 trials with EEG artifacts were removed, resulting in a clean dataset of 133,683 trials across 598 sessions. Sessions were divided into "high" and "low" performing groups using a k-means clustering algorithm ( $k=2$ ) based on the proportion of correctly classified MI trials per session. This resulted in 250 sessions in the "high" performing group and 348 in the "low" performing group.

#### 4.2 Quantification of Motor Imagery Dynamics

The data from [Stieger et al. \(2020\)](#) were pre-processed by the original authors, including artifact marking and a bandpass filter between 0.1 and 100 Hz. The raw data were further filtered to capture only the Mu band (8-13Hz) over the left and right sensorimotor regions, which is associated

with capturing an ERD during MI. The ERS, primarily captured by the beta band, was not considered to avoid increasing the study's complexity, as disentangling ERS and ERD would be necessary to prevent positive and negative synchronization effects from canceling each other out. The EEG data in the Mu band for the Rest and MI phases were squared to obtain power. Bandpassing and squaring were chosen for computational efficiency over methods like Time-Frequency analysis. The Rest phase power was averaged and used as a baseline for the MI phase. ERD values, as quantified by the relative increase/decrease of power for each sample during MI compared to the baseline, were extracted using a formula 1 and 2 (Pfurtscheller & Da Silva, 1999).

$$ERD_{C3} = \frac{PowerMI_{C3} - PowerREST_{C3}}{PowerREST_{C3}} * 100 \quad (1)$$

$$ERD_{C4} = \frac{PowerMI_{C4} - PowerREST_{C4}}{PowerREST_{C4}} * 100 \quad (2)$$

These values are further averaged over the samples within each trial, giving the average of Mu-band suppression within the MI phase.

#### 4.3 Parameters for Multifractal Detrended Fluctuation Analysis

MFDFA metrics are derived from the raw EEG spectrum (0.1 - 100 Hz) using the R package FractalRegressions (Likens & Wiltshire, 2023). The sensitivity of MFDFA estimations necessitates precise parameter settings. The q-range, weights the time series fluctuations, where positive q-values highlight larger fluctuations, while negative values relate to smaller fluctuations. A range of -5 to 15, is based on the EEG analysis in Gaurav et al. (2021). This range prevents computational errors and the dominance of extreme fluctuations in smaller timeseries typical for EEG. Furthermore a detrending order of 2 was used, which is a sufficient detrending order according to Gaurav et al. (2021).

##### 4.3.1 Minimal scale range

The scale range used in MFDFA impacts the calculated estimates. The minimal scale affects the granularity of the analysis and how small-scale fluctuations are quantified. The minimal value should be based on the fastest significant frequency component in the data, and its sampling frequency (Ihlen & Vereijken, 2010). Since both the Rest and MI data were bandpassed at 100Hz, the fastest significant frequency component is at 100Hz. Considering a sampling frequency of 1000Hz, we divide the sampling frequency by the fastest frequency component, setting a minimal

scale of 10. This ensures that each segment captures at least one full cycle of the fastest dynamics, while ensuring that the analysis is stable and that the estimation of local Root Mean Square (RMS) fluctuations avoids random noise that might appear significant in smaller segments.

#### 4.3.2 Maximal scale range

Conversely, the maximal scale, typically between 1/4th and 1/10th of the total data points (Ihlen & Vereijken, 2010), ensures there are enough segments for robust statistical analysis, influencing the ability to observe long-range correlations and larger structural patterns within the data. The MI period has varying signal lengths based on the time that a participant need to complete the MI task, which complicates things slightly. One approach could be to have varying maxima for each trial. This would give the most tailored MFDFA analysis for each trial, however, this can lead to inconsistencies when comparing the results across different trials, sessions or participants. As such a comparison is one of the main goals of the study, an alternative approach is used, namely to select a common maximal scale for all trials. In this case the common maximal scale is based on the median of signal lengths, which was 3120 samples. Therefore, the maximum scale for all MI trials was set to 312 (1/10th). The downside is that this may limit the ability to detect scale-dependent features for large time periods, as their analysis will be constrained to the smaller maximal scale. Alternatively, if the signal is very short, the estimate might have a higher variance, as there are too few segments to compare for robust statistical analysis (Ihlen & Vereijken, 2010). The maximal scales of the Rest period, which consists of 2000 samples, were also set to 312 to ensure similar maximal scales between MI and Rest periods. While the maximal value is not ideal for the Rest period, it still falls within the typical range of 1/10th to 1/4th.

#### 4.4 Comparing multifractality between Rest and MI for performance groups

The differences between the MFDFA metrics during the Rest and MI periods are compared between two performance groups by analyzing the singularity spectra and the curves of Generalized Hurst exponents across different statistical moments ( $q$ ). Three main components of MFDFA are examined to quantify the degree and strength of multifractality:  $MFDFA_{Width}$ , which measures the width of singularity strengths ( $h$ ) during MI;  $MFDFA_{Width-Rest}$ , the width during rest; and  $MFDFA_{Width-Diff}$ , the difference in width between MI and rest. By subtracting the multifractal width during MI from that during Rest, we create a baselined width that indicates the change in

complexity directly caused by imagining a direction. The range of generalized Hurst exponents is the second metric that is examined ( $\delta H(q)$ ) and indicates the range of different scaling exponents over different scales. Lastly, the skewness of the multifractal spectrum is visually examined, which represents the asymmetry and potential long-tailed distributions in the underlying data, providing insights into the predominance of large or small fluctuations in the time series. Analyzing these plots and metrics will give an overall insight into the multifractal dynamics of MI compared to Rest, helping to answer RQ<sub>1</sub>, as well as providing the differences between the performance groups, providing insights into RQ<sub>2</sub>.

#### 4.5 Lateralization

Next, the phenomenon of lateralization in ERD, MFDFA<sub>Width</sub>, and MFDFA<sub>Width-Diff</sub> metrics were explored. These metrics were compared between contralateral and ipsilateral channels. For instance, when participants imagined left-side movement, C<sub>4</sub> channel activity was contralateral, while C<sub>3</sub> channel activity was ipsilateral. To test for differences between laterality for all three metrics, three bonferroni corrected Wilcoxon signed rank tests were employed, given the non-normally distributed metrics.

After testing for differences in the metrics between hemispheres, the degree and direction of lateralization were examined using the LI. The LI, as described in [Doyle et al. \(2005\)](#), can be quantified as:

$$LI = \frac{(Power_{C3Left} - Power_{C4Left}) + (Power_{C4Right} - Power_{C3Right})}{2} \quad (3)$$

Applying the same formulaic structure to MFDFA<sub>Width</sub> and MFDFA<sub>Width-Diff</sub>, gives us the degree of lateralization of (multifractal) complexity (formula 4). Note that for clarity, both MFDFA<sub>Width</sub> and MFDFA<sub>Width-Diff</sub> were abbreviated as MFDFA.

$$LI_{MFDFA} = \frac{(MFDFA_{C3Left} - MFDFA_{C4Left}) + (MFDFA_{C4Right} - MFDFA_{C3Right})}{2} \quad (4)$$

For each LI metric, differences between high and low performance groups were visually inspected through boxplots and tested for significance. Moreover, all LI's for both performance levels were statistically compared to 0, using Bonferroni corrected Wilcoxon signed-rank test, to verify whether the lateralization differed from a bilateral interaction. A metric statistically different from 0 would indicate the presence of a dominating hemisphere.

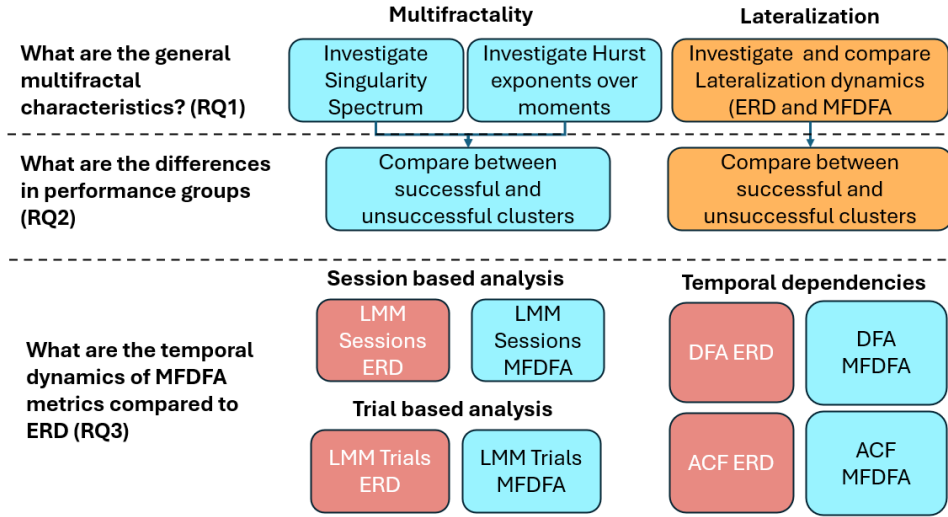


Figure 3: General overview of analysis steps and their corresponding RQ.

#### 4.6 Temporal effects on ERD and MFDFA

To investigate the temporal effects of both ERD and MFDFA a mix of DFA, ACF, and linear Mixed-effect models were employed. Specifically inter Session, and inter trial dynamics were investigated, providing insights regarding RQ3.

##### 4.6.1 Session based analysis

To investigate changes over sessions, six different linear mixed-effect models were employed, each tailored to a specific metric of interest. The metrics analyzed included task accuracy, as well as,  $MFDFA_{Width}$ ,  $MFDFA_{Width-Diff}$ , and ERD values. The ERD-values were first Log-transformed, given their long-tailed distribution (Appendix 9). A random effect is introduced for Subjects, in order to account for inter subject variability. The following linear mixed-effect models were used:

$$\text{Log}(ERD) \sim \text{Session} + (1|\text{Subject}) \quad (5)$$

$$MFDFA_{Width} \sim \text{Session} + (1|\text{Subject}) \quad (6)$$

$$MFDFA_{Width-Diff} \sim \text{Session} + (1|\text{Subject}) \quad (7)$$

$$\text{Accuracy} \sim \text{Session} + (1|\text{Subject}) \quad (8)$$

For each linear mixed-effect model, the Estimate and p-values were extracted to assess the significance and magnitude of the changes over sessions.

#### 4.6.2 Long term dependency in ERD and MFDFA

Detrended Fluctuation Analysis was used to investigate the long range temporal correlations within sessions. Each trial has a value for ERD or  $MFDFA_{Width}$  or  $MFDFA_{Width-Diff}$ , which can be interpreted as a timeseries, where each trial is a time point within the analysis (Perquin et al., 2023). By calculating DFA over trials for each session, we can track the long term dependency within each session, and compare them between sessions. For each session, the DFA exponent was computed for the ERD,  $MFDFA_{Width}$ ,  $MFDFA_{Width-Diff}$  metrics. The scales that were used are on a log scale in the range of 4 to 52, as the time series were short (225 samples). A detrending order of 2 was used, based on visual inspection of consistency of scaling exponents derived from the log transformed root mean squares of the detrending functions. For a detrending order of 2, the scaling exponent derived from the log\_rms plot was consistent across scales, suggesting that the detrending effectively normalized the data. The DFA exponent extracted from this analysis indicates the presence of LTC, with values typically between 0.5 (indicating no correlation/random process) and 1.5 (indicating a highly correlated process). DFA values were visually compared between ERD,  $MFDFA_{Width}$ , and  $MFDFA_{Width-Diff}$ , for each session between both high and low performing clusters.

#### 4.6.3 Autocorrelation

ACF analysis was utilized to estimate the degree of autocorrelation within the data across different lags, where each lag represents a subsequent trial. For instance, a lag of 1 indicates the correlation between a metric's value at a given trial and its value at the next trial, while a lag of 2 represents the correlation between the metric's value at a given trial and its value two trials ahead, and so forth. This analysis helps in understanding the persistence or memory in the data by examining how the values of a metric are dependent on previous trials. Significant autocorrelations at specific lags indicate how past trials influence subsequent ones, possibly revealing patterns such as trends or cycles in the data. ACF plots were generated and compared between session for ERD-,  $MFDFA_{Width}$ -, and  $MFDFA_{Width-Diff}$ -metrics.

#### 4.6.4 *Inter-trial variability*

To investigate inter-trial variability, LMMs were employed to analyze how ERD, MFDFA<sub>Width</sub>, MFDFA<sub>Width-Diff</sub> change across trials. Moreover, the MFDFA<sub>Width</sub> during rest was investigated to possibly investigate changes in cognitive states such as fatigue. This analysis aimed to understand the fluctuations and patterns within sessions, providing insights into the consistency and variability of these metrics across individual trials. Similar to the Sessional LMM analysis, difference between subjects are accounted for by introducing a Random effect.

$$\text{Log(ERD)} \sim \text{Trial} + (1|\text{Subject}) \quad (9)$$

$$\text{MFDFA}_{\text{Width}} \sim \text{Trial} + (1|\text{Subject}) \quad (10)$$

$$\text{MFDFA}_{\text{Width-Diff}} \sim \text{Trial} + (1|\text{Subject}) \quad (11)$$

$$\text{MFDFA}_{\text{Width-Rest}} \sim \text{Trial} + (1|\text{Subject}) \quad (12)$$

## 5 RESULTS

This study applied MFDFA to EEG signals recorded during MI training to investigate their non-linear properties. The first research question explored the multifractal characteristics of EEG signals during MI and their relation to established neural mechanisms by examining MFDFA metrics, including the degree of multifractality and lateralization (see sections 5.1 and 5.2). For RQ2, these metrics were compared between high and low-performing groups to assess performance-related differences in MI-related brain activity (see sections 5.1 and 5.2). The third research question examined the temporal evolution of multifractal properties during MI training over multiple sessions, addressing BCI inefficiency through inter-trial and inter-session variability (see section 5.3). This included a comparison with traditional linear descriptors to evaluate MFDFA's potential advantages in capturing dynamic changes associated with MI practice. The following sections detail the findings for each research question, highlighting multifractal characteristics, performance-based differences, and the temporal evolution of EEG signals during motor imagery tasks.

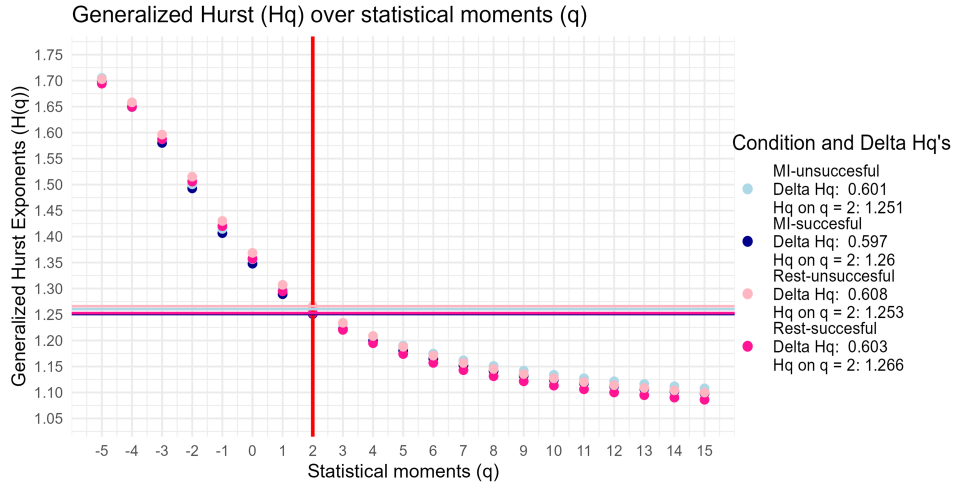


Figure 4: Generalized Hurst exponents over different statistical moments of  $q$ . Similar to the Singularity spectrum, the dark points (Dark pink, and Dark blue), indicate the aggregate of all successful trials, whereas light points (Light pink and Light blue) indicate the aggregate of all unsuccessful trials

### 5.1 Multifractal Analysis

By comparing the multifractal characteristics of EEG signals during rest and MI, specific changes in brain activity associated with the cognitive process of imagining movement can be identified. This comparison helps establish a baseline for multifractal complexity, allowing the unique aspects of MI to be pinpointed and potentially improving the accuracy and efficacy of BCI applications. The differences between Rest and MI were compared for both performance clusters. The singularity spectrum in 5 shows the singularity dimensions  $D(h)$  against the singularity strength  $h$  for four conditions: MI-successful, MI-unsuccessful, Rest-successful, and Rest-unsuccessful. For the same conditions, figure 4 shows the Generalized Hurst exponent ( $H(q)$ ) over different statistical moments ( $q$ )

#### 5.1.1 Generalized Hurst exponents

Figure 4 shows the  $H(q)$  values over statistical moments  $q$  for aggregates of successful and unsuccessful trials for both MI and Rest phases. For all aggregates, there is variability in  $H(q)$  values across different  $q$  values. This variation indicates multiple scaling behaviors within the signal, reflecting the presence of multifractal structures. The spectrum  $\Delta H(q)$  values are 0.601 for MI-unsuccessful, 0.597 for MI-successful, 0.608 for Rest-unsuccessful, and 0.603 for Rest-successful, showing close similarity in multifractal behavior with a marginally taller spectrum for unsuccessful

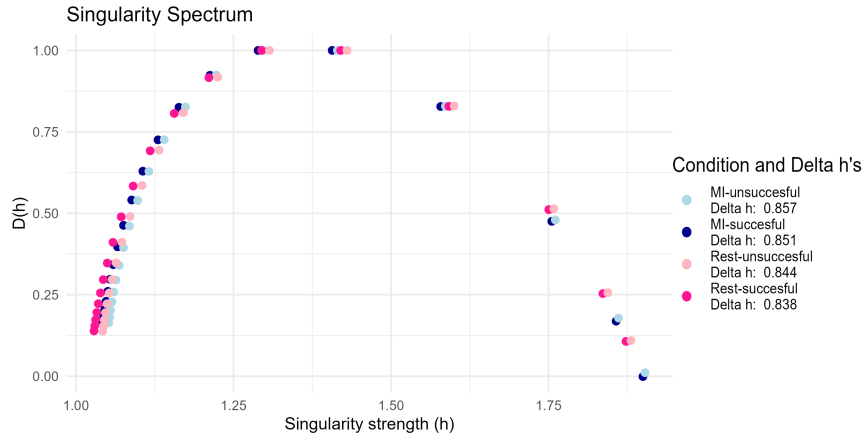


Figure 5: Singularity spectrum of EEG activity during rest (pink) and MI (blue). The dark points (Dark pink, and Dark blue), indicate the aggregate of all successful trials, whereas light points (Light pink and Light blue) indicate the aggregate of all unsuccessful trials

aggregates. This similarity in  $\Delta H(q)$ , as well as the overall similarity of the plots, suggests that the multifractal properties of the motor imagery data are relatively consistent across the aggregates. Notably, for both MI and Rest, the unsuccessful trials have higher  $H(q)$  values across all  $q$ 's compared to successful trials, indicating more persistent and less variable brain activity during unsuccessful trials.

### 5.1.2 Singularity Spectrum

Figure 5 shows the Singularity spectrum, which show the distribution of scaling properties present in the signals during MI and Rest for successful and unsuccessful trials. Higher Singularity strength ( $h$ ) show more regularity, and big fluctuations, whereas lower singularity strength indicate the presence of small fluctuations. For all aggregates, the structure of the singularity spectrum was very similar, indicating that the fluctuations exhibit consistent scaling behaviors across the different time scales. Furthermore, the singularity spectrum of both MI-successful and MI-unsuccessful were asymmetric, with left skewness, indicating that the system is characterized by multifractality with more pronounced smaller fluctuations (high degree of "roughness"), and that it is insensitive to local fluctuations with large magnitudes (Ihlen & Vereijken, 2010). Multifractal dimension or  $D(h)$  shows for differing levels of  $h$  how impactful these fluctuations are for the timeseries.

The multifractal width ( $\Delta h$ ) was 0.857 for MI-unsuccessful and 0.851 for MI-successful, while resting conditions had widths of 0.844 for unsuccessful

and 0.838 for successful trials. A Holm-corrected Wilcoxon signed-rank test indicated that successful and unsuccessful trials were significantly different (for both MI and Rest), and also that Rest and MI were statistically different (for both performer groups), see table 1. However, the effect sizes (Cohen's d) were all smaller than 0.1, indicating very small differences (see Table 1). These results suggest that the MI phase had slightly higher multifractal widths compared to Rest phase and that successful trials had lower widths compared to unsuccessful ones.

Test	Adjusted_p_value	Effect_Size	Effect_Size_Class
MI successful vs MI unsuccessful	<0.001	0.014	Very Small
Rest successful vs Rest unsuccessful	<0.001	0.011	Very Small
Successful Rest vs Successful MI	<0.001	0.038	Very Small
Unsuccessful Rest vs Unsuccessful MI	<0.001	0.040	Very Small

Table 1: Results of statistical tests with adjusted p-values and effect sizes.

## 5.2 Lateralization

The following section reports on the results of the lateralization analysis, which is a critical aspect of classifying MI. By comparing contralateral and ipsilateral brain activity, as well as examining the LI, the aim is to determine the degree and direction of lateralization.

Table 2: Statistical test between Lateral Hemispheres between ERD, MFDFA\_Width, and MFDFA\_Width\_Diff

Metric	P-value	W
ERD	< 0.001	919158005
MFDFA_Width	< 0.001	9333369683
MFDFA_Width_Diff	< 0.001	9349165179

To test whether there were statistical differences in ERD, MFDFA<sub>Width</sub>, and MFDFA<sub>Width-Diff</sub> between contra- and ipsilateral hemispheres, 3 bonferroni corrected Wilcoxon signed rank tests were employed. All 3 tests were significant ( $p < 0.001$ ), see table 2. This suggests that for all three metrics there is evidence for ispi- or contralateralization.

To further investigate the degree of lateralization, the LI's from Motor Imagery across different performance groups and metrics is illustrated in the three sub-plots presented in Figure 6. For all three metrics, the High performing group seems to be contralaterally dominated, with some outliers having bi, or ipsilaterally dominated interactions. The low performers seem to have an LI around 0, indicating that no hemisphere is dominating

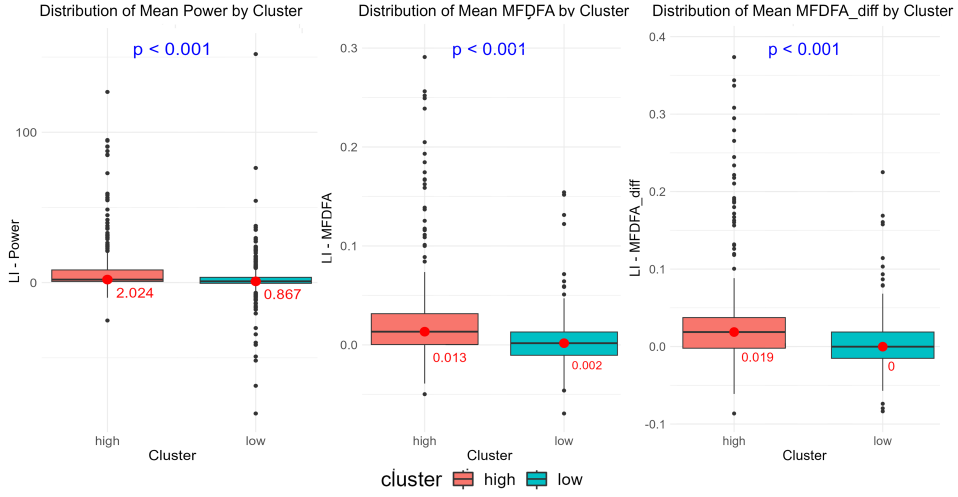


Figure 6: Comparison of high and low clusters between Lateralization Indexes of ERD,  $MFDFA_{Width}$  and  $MFDFA_{Width-Diff}$ , showing a contralaterally dominating dynamics for high performers, and bilateral dynamics for low performers in all metrics

the MI interaction. A statistical test between the two clusters further shows this difference, where there is a significant difference between Low and High performing groups ( $p < 0.001$ ). Furthermore, there seems to be a large amount of (positive) outliers for all metrics, indicating that there is quite some variation regarding the degree at which the interaction is contralaterally dominated. Furthermore, all LI-indexes of high performers differ statistically from 0,

Table 3 shows whether LI based on Power,  $MFDFA_{Width}$  and  $MFDFA_{Width-Diff}$  are different from 0. A Wilcoxon signed rank test confirms that for all metrics, high performers statistically differ from 0. Meanwhile, for low performers, only power differed statistically from zero.

Table 3: Adjusted p-values from Wilcoxon Tests, comparing LI indexes to be greater than 0

Cluster	Power	$MFDFA_{Width}$	$MFDFA_{Width-Diff}$
High	$P < 0.001$	$P < 0.001$	$P < 0.001$
Low	$P < 0.001$	$P = 0.922$	$P = 1$

Table 4: Adjusted p-values from Wilcoxon Tests, comparing LI indexes to be greater than 0

### 5.3 Temporal dynamics

The linear mixed models were fitted to assess the effect of Session on various dependent variables, accounting for random intercepts by Subject (see Table 5). The intercepts for all models were significantly different from zero (all p-values  $< .001$ ), indicating substantial baseline levels for the dependent variables. Moreover, the effect of Session was significant in all models (all p-values  $< .001$ ). Surprisingly, the ERD estimate has a baseline of 975.868, which decreases on average by 9.900 per session. The MFDFA<sub>Width</sub> starts at an estimate of 0.874, which increases on average by 0.001 per session. On the contrary the MFDFA<sub>Width-Diff</sub> model has a baseline of 0.016, which decreases on average by 0.001. When interpreting these changes in MFDFA, it should be considered that a seemingly tiny change, can already be quite a difference in the multifractal behaviour in the original signal. Lastly, the Accuracy model demonstrated that sessions positively affect accuracy. The accuracy at session 1 is on average 54.5%, with an increase of 0.7% per session of training, reaching an average accuracy of 62.2% after 11 sessions.

Model	Term	Estimate	Std. Error	Statistic	p-value	Conf. Low	Conf. High	R squared
ERD - Session	(Intercept)	975.868	99.805	100.479	< 0.001***	836.401	1136.108	0.04621785
ERD - Session	Session	-9.900	0.990	-8.357	< 0.001***	-9.901	-9.899	0.04621785
MFDFA <sub>Width</sub> - Session	(Intercept)	0.847	0.010	86.003	< 0.001***	0.827	0.867	0.13166355
MFDFA <sub>Width</sub> - Session	Session	0.001	0.000	5.665	< 0.001***	0.000	0.001	0.13166355
MFDFA <sub>Width-Dif</sub> - Session	(Intercept)	0.016	0.004	4.602	< 0.001***	0.009	0.023	0.01066807
MFDFA <sub>Width-Dif</sub> - Session	Session	-0.001	0.000	-4.324	< 0.001***	-0.001	0.000	0.01066807
Accuracy - Session	(Intercept)	0.545	0.017	32.177	< 0.001***	0.511	0.579	0.34737303
Accuracy - Session	Session	0.007	0.001	5.434	< 0.001***	0.004	0.009	0.34737303

Table 5: Summary of Session Models

#### 5.3.1 Detrended Fluctuation Analysis

Figure 7. illustrates the mean DFA scaling exponent values across trials of different sessions for three distinct metrics: ERD, MFDFA<sub>Width</sub>, and MFDFA<sub>Width-Dif</sub>. The dotted black line indicates the border of alpha = 0.5, indicating no LTC, and suggesting a random walk-like behaviour. Higher DFA value indicate stronger LTCs, meaning that values at the start of a session have a more substantial influence on values later in that session, reflecting more persistent temporal patterns in the data. For both ERD and MFDFA<sub>Width</sub>, the DFA alpha value is around 0.55, with large error bars, indicating that there are large differences in the alpha exponents between participants. MFDFA<sub>Width-Dif</sub> shows slightly less variation in alpha exponents between participants, however, the mean alpha exponent is around 0.5, indicating no LTC.

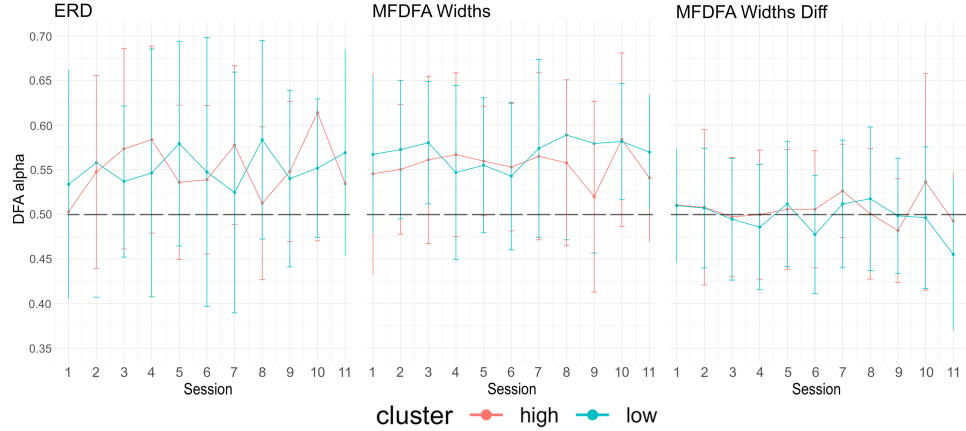


Figure 7: Detrended Fluctuation Analysis of trials per session, with an error bar showing the distribution between participants. The left most plot shows DFA values over sessions for ERD values, the middle plot shows  $MFDFA_{Width}$ , and the right plot shows  $MFDFA_{Width-Diff}$

### 5.3.2 Autocorrelation

The ACF analysis for ERD, MFDFA widths, and  $MFDFA_{Width-Diff}$  across sessions and participants are shown in Figure 8. The leftmost ACF plot shows the autocorrelation of ERD values over trials for 11 different sessions. Interestingly, high session counts (specifically session 6, 7, 9, 10, and 11) show ACF values that do not exceed the 95% confidence interval marked by the dotted red line, making them indistinguishable from 0 AC. Lower sessions (Session 1 to 5), as well as session 8 have a few lags where autocorrelation is around 0.005 and 0.02, indicating very low, but significant autocorrelation.

The second ACF plot shows ACF values of  $MFDFA_{Width}$ . Here all sessions have significant autocorrelation values up to a lag of 11. Autocorrelation levels are higher than that of ERD, with values between 0.025 and 0.075, indicating that there is a small but noticeable correlation between consecutive trials within the same session. This suggests that the multi-fractal width values have a degree of consistency or pattern over the trials, implying that the changes in MFDFA width are not entirely random but have temporal structure to it.

The third ACF plot shows anti-correlation at lag 1, indicating that high  $MFDFA_{Width-Diff}$  in one trial are likely followed by lower values in the next trial (and vice versa). Interestingly, the  $MFDFA_{Width-Diff}$  follows similar patterns with respect to AC values as the AC values from the ERD. (Figure 1) indicates a small but significant negative autocorrelation at lag 1, where

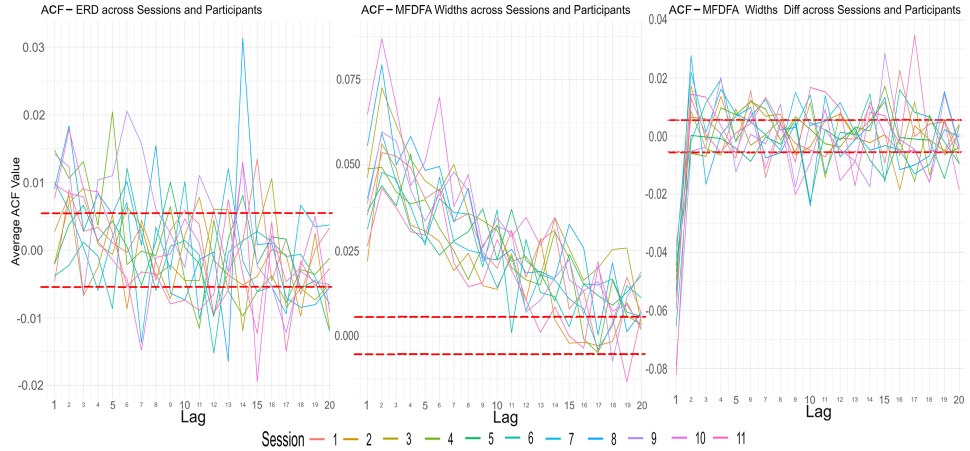


Figure 8: ACF plots for ERD, MFDFA<sub>Width</sub>, and MFDFA<sub>Width-Diff</sub> showing the degree of autocorrelation over different lags (trials)

high ERD values in one trial are likely followed by lower values in the next, with overall low correlation persisting up to lag 18.

### 5.3.3 Inter-trial variability

The linear mixed models were fitted to assess the effect of Trials on ERD, MFDFA<sub>Widths</sub>, MFDFA<sub>Widths-Diff</sub>, and MFDFA<sub>Widths-Rest</sub>, accounting for Subject variability (see Table 6). The intercepts for all models were significantly different from zero (all p-values < .001), indicating substantial baseline levels for the dependent variables.

The effect of Trials was significant in several models. The ERD model demonstrated a significant effect of trials (Estimate = -9.899, SE = 0.990, p < .001), indicating a decrease in ERD values over trials. The MFDFA<sub>Widths</sub> model also showed a significant effect of trials (Estimate = 0.00002, SE = 0.000003, p < .001), indicating a very small increase in multifractal complexity over trials. Additionally, the MFDFA<sub>Widths-Rest</sub> model exhibited a significant effect of trials (Estimate = 0.00003, SE = 0.000003, p < .001), indicating an increase in multifractal complexity during rest periods over trials. Interestingly, the MFDFA<sub>Width-Diff</sub> model did not show a significant effect of trials (Estimate = -0.000006, SE = 0.000004, p = .137). This potentially indicates that since both MFDFA<sub>Widths</sub> and MFDFA<sub>Widths-Rest</sub> increase, but not the difference between them (MFDFA<sub>Width-Diff</sub>), the overall increase in multifractal complexity might be driven by a change in the baseline (background activity) rather than changes in multifractal width that are only present during the MI task.

Model	Term	Estimate	Std. Error	Statistic	p-value	Conf. Low	Conf. High	R <sup>2</sup>
ERD - Trials	(Intercept)	1190.937	99.815	103.926	< 0.001***	1024.796	1381.620	0.05006356
ERD - Trials	Trial	-9.899	0.990	-36.045	< 0.001***	-9.898	-9.898	0.05006356
MFdfaWidths - Trials	(Intercept)	0.847	0.010	85.982	< 0.001***	0.827	0.867	0.13216965
MFdfaWidths - Trials	Trial	0.00002	0.000003	7.184	< 0.001***	0.00001	0.00003	0.13216965
MFdfaWidth-Diff - Trials	(Intercept)	0.014	0.004	3.860	< 0.001***	0.007	0.021	0.01052938
MFdfaWidth-Diff - Trials	Trial	-0.000006	0.000004	-1.485	0.137	-0.001	0.00001	0.01052938
MFdfaWidths-Rest - Trials	(Intercept)	0.833	0.009	89.351	< 0.001***	0.814	0.852	0.10853015
MFdfaWidths-Rest - Trials	Trial	0.00003	0.000003	8.635	< 0.001***	0.00002	0.00003	0.10853015

Table 6: Summary of Trials Models

## 6 DISCUSSION

The primary objective of this thesis was to delve deeper into the multi-fractal characteristics of EEG signals during MI, moving beyond the mere application of features in classifiers and trying to better understand how non-linear descriptors can help in understanding brain activity. Specifically, RQ1 sought to understand the multifractal characteristics of EEG signals during MI. Meanwhile, RQ2 aimed to investigate whether MFDFA metrics differ based on participant performance. And lastly, RQ3 focused on understanding how the multifractal properties of EEG signals evolve with motor imagery training and how these changes compare to traditional linear descriptors.

### 6.1 Multifractal Analysis

To answer RQ1, a multifractal analysis was performed to provide a general understanding of multifractal characteristics during MI. The analysis revealed that EEG signals during MI and rest phases exhibited consistent scaling behaviors across all conditions. The H(q) over q plot, in combination with the singularity spectrum indicated that fluctuations exhibit multifractal structures with a predominance of small fluctuations, showing more regularity in MI phases. These initial findings are consistent with previous studies showing that brain activity shows multifractality (Gaurav et al., 2021; Paul et al., 2015; Sikdar et al., 2018).

#### 6.1.1 Multifractal measures

A more unique finding relates to the differences in multifractal width between phases, which were slightly higher for the MI phase compared to rest. This suggests that MI phases have a slightly broader range of scaling exponents, characterizing a more complex signal. Additionally, the range of Generalized Hurst exponents ( $\Delta H(q)$ ) was smaller in MI compared to rest. This means that although the MI phase exhibits more variability in the magnitude of fluctuations, there was more consistency

in how these fluctuations scale across different statistical moments. This indicates that, while the brain activity during MI shows more diverse patterns of fluctuations, these patterns follow a more uniform scaling behavior, reflecting stable and coherent long-range correlations during the cognitive process of imagining movement.

#### *6.1.2 Multifractal measures interpreted through the lens of ERD and ERS*

These findings can be interpreted through the dynamics of the ERD as described in Pfurtscheller and Da Silva (1999) and Solodkin, Hlustik, Chen, and Small (2004). During ERD, there is a reduction in the power of specific frequency bands, allowing for more complex and variable patterns of brain activity. In this case, small-scale fluctuations, such as minor variations in neural firing rates, have a substantial impact on large-scale fluctuations, which are characterized by the desynchronization of brain activity. This is reflected by the increase of multifractal width between MI and Rest. A higher multifractal width suggests that the time series has a more complex structure with a greater variety of local scaling behaviors, which indicates that there are more distinct regions with differing levels of variance. This is congruent with findings of linear metrics, as it has become apparent that variance is a viable metric for the calculation of the ERD/ERS (Pfurtscheller, 2000).

Despite the increased local variability, the overall scaling properties became more consistent across different statistical moments, as indicated by the smaller  $\Delta H(q)$ . Within the scope of this literature review, there were no other papers reporting similar dynamics in linear metrics. Nonetheless, a potential interpretation is that during MI, the EEG signal becomes dominated by (de)synchronization processes. This might makes the signal less complex because the relationship between small- and large-scale fluctuations becomes stronger, which reduces the influence of other interactions and, consequently, the range of Hurst exponents. If this is the case, this metric could potentially be used to model the degree of (de)-synchronization, possibly providing a new metric for capturing MI, which doesn't relate to the linear increase in power or variance, but rather by the interactions within the signal. A future study should investigate whether machine learning models could benefit from including this feature.

#### *6.2 Differences in multifractal width between successful and unsuccessful trials*

To provide answers to RQ2, the differences in multifractal width between successful and unsuccessful trials were compared, showing higher multi-

fractal width, and a lower range of Hq's for unsuccessful trials in both MI and Rest periods.

One interpretation is that the higher multifractal widths in unsuccessful conditions could relate to cognitive load and distractions. Studies have shown that during mind wandering or less focused states, the complexity of EEG signals, measured using for example multiscale entropy (MSE), increases, compared to states of focused attention ([Lu & Rodriguez-Larios, 2022](#); [Proteau-Lemieux et al., 2021](#)). Higher multifractal width indicates more variability and complexity in neural activity, which might suggest that during unsuccessful trials, participants experience increased cognitive interference or are more distracted. This increased complexity could lead to less effective motor imagery, as the brain's resources are spread across various competing neural processes rather than being concentrated on the MI task.

Another observation is that the difference in multifractal width between successful and unsuccessful trials is similar in MI and Rest. This indicates that there is already a difference in brain state between successful and unsuccessful trials prior to the MI phase. This is congruent with the body of literature suggesting that the neural groundwork laid during rest can significantly influence the subsequent task performance ([Stieger et al., 2020](#)). This suggests that multifractal width could potentially be used to differentiate between background activity and task activity (more on this in section 6.6).

### 6.3 *Lateralization of the ERD*

The degree of lateralization was also contrasted between linear and non-linear metrics, to provide further answers to both RQ1 and RQ2. Interestingly, the contralateralization dynamics were the same for all metrics, where the contralateral hemisphere shows greater desynchronization for high performers for all metrics. On the contrary, Low performers have significantly less contralateral activity. This aligns with the main body of literature, suggesting Power is contralateral in high performers, and less so in low performers, while also providing evidence that the multifractal width shows similar patterns. These findings provide answers to RQ1 and RQ2, suggesting that the general multifractal characteristics are similar as the linear (ERD) metrics, and likely allow for MI classification, given the contralateral nature. Moreover, all metrics, but especially the lateralization of power, suggest a long tailed distribution, which highlight the inter-subject/session variability ([Zhang et al., 2020](#)).

It is important to highlight that MFDFA was computed for the full EEG spectrum (0.1 Hz - 100Hz), which contain both mu-band suppression,

characterized by the ERD, as well as changes in the beta frequency band, caused by the ERS. The ERS involves the re-synchronization of neuronal activity, typically observed in the ipsilateral hemisphere and associated with the inhibition of movement. During ERS, MFDFA<sub>Width</sub> is likely to decrease due to the stabilization of large-scale fluctuations and suppression of small-scale variations, leading to less variable brain activity. When considering the LI of MFDFA<sub>Widths</sub>, a reduction in MFDFA widths in the ipsilateral hemisphere which consequently would contribute to a contralaterally dominating interaction. Thus both ERD and ERS contribute to the LI of MFDFA. Future research could disentangle multifractality of ERS and ERD mechanics by using amplitude envelopes of the appropriate frequency bands. This could further back up the interpretation that was made previously regarding the influence of the ERD/ERS on multifractal width (as well as  $\Delta H(q)$ ).

The absence of lateralization in multifractal width among low performers suggests that these individuals do not show contralateralization, addressing RQ2 of this thesis. This suggests that there is a lack of appropriate neural activity generation, rather than a classifier issue. While the multifractal width is not necessarily contralateral in low performers, this doesn't mean that they cannot have generated some contralateral activity. It is possible that there are changes in the interactivity between scales, that do not reflect in the range of  $h$ . A followup work should investigate whether the difference in  $\Delta H(q)$  between rest and MI also exhibits contralateral dynamics, and whether they are present in high and low performers.

#### 6.4 Temporal Analysis

The temporal analysis aimed at providing answers to RQ3, by doing a sessional and trial based analysis by employing LMM's, DFA, and ACF.

First of all, the sessional analysis revealed a significant improvement in the accuracy metric over the course of 11 sessions of MI training, suggesting that learning took place. Moreover, metrics describing MI had significant changes over sessions. Surprisingly, the magnitude of the ERD decreased over sessions, showing less power differences compared to rest, which is incongruent with previous literature (Hashimoto, Ushiba, Kimura, Liu, & Tomita, 2010). It is possible that this is a result of the extremely long tail in the distribution of ERD metrics (Appendix 9). The ERD values were log-transformed allowing for the LMM to fit, however, this means that the extreme values were included in the baseline of the model, possibly incorrectly changing the results. Considering that the MFDFA values did not have a long tailed distribution, we can continue interpreting the non-linear models.

$MFDFA_{Width}$  had an increase in multifractal width, indicating that the multifractal complexity increases over the course of MI training. Contrarily, the  $MFDFA_{Width-Diff}$ , shows a decrease in multifractal width. This is a very interesting finding, as it suggests that the overall complexity of brain activity (including background activity), increases, whereas the complexity of the activity solely related to MI decreases. The decrease in  $MFDFA_{Width-Diff}$  is in line with the hypothesis of Hebbian learning, which is often summarized as "cells that fire together wire together" suggests that repeated practice strengthens specific neural pathways, enhancing their efficiency and specificity (Gerstner, 2011). This efficiency can be interpreted as a decrease in the complexity of the brain acitvity during the MI task.

The increase in multifractal width for  $MFDFA_{Width}$  contrasted to  $MFDFA_{Width-Diff}$  is surprising, and raises questions about neural priming. Priming refers to the enhancement of motor system readiness due to repeated mental rehearsal of movements, which typically leads to more efficient neural processing over trials (Stoykov, Corcos, & Madhavan, 2017). This can be seen as the decrease of necessary complexity during  $MFDFA_{Width-Diff}$ .

### 6.5 *Temporal dependency*

The results from the ACF and DFA analyses provide insights into the short and long-term dependencies of  $MFDFA_{Width-Diff}$ , ERD, and  $MFDFA_{Width}$ . The ACF revealed that both ERD and  $MFDFA_{Width-Diff}$  exhibit little to no significant short-term autocorrelation, indicating that closely timed trials do not influence each other. This is incongruent with previous literature for ERD, which suggests significant short and long-term correlations during physical movement. This discrepancy might be due to ERD in this study being caused by imagined movement. In contrast,  $MFDFA_{Width}$  shows significant autocorrelation for up to 11 trials, indicating short-term dependencies and suggesting stable neural responses over short periods.

The DFA analysis revealed LTC across the entire session. ERD and  $MFDFA_{Width}$  exhibit similar  $\alpha$  exponents, indicating similar degrees of LTC, whereas  $MFDFA_{Width-Diff}$  shows random walk-like behavior and an absence of LTC. This suggests that the difference of  $MFDFA_{Width-Rest}$  and  $MFDFA_{Width}$ , effectively baselines background brain activity and noise. However, a random walk-like behavior could also entail that the variable is semi-random, which might mean it has poor predictive power. Future studies could explore the effect of this on inter-trial variability. Lastly, considering  $MFDFA_{Width}$  has similar LTC, and higher autocorrelation than the ERD metric, it is possible that this metric is better able to capture longer term dynamics, such as attention.

While the temporal analysis did not reveal differences between performance groups, this analysis has provided a first glance at the temporal dependencies of multifractal measures, which reveal that MFDFA<sub>Width</sub> and MFDFA<sub>Width-Diff</sub> have different temporal structures, highlighting the effect of the general brain state on these metrics describing MI interaction. Future work can investigate whether a combination of these metrics could be used to reduce trial-invariant metrics, reducing effects of attentional states on the results of MI classification.

### 6.6 *Inter-trial variability*

The observed differences in ERD over trials are similar to those found over sessions, indicating that power differences between MI and rest become less pronounced with an increasing number of trials. Similar to the sessional analysis, this could be due to the long tail of the distribution. Alternatively, it is possible that participants grow tired over trials, inhibiting their ability to create a high ERD. Future research could look into a modeling approach that better suits this distribution, or apply standardization strategies to make sure outlying participants/trials do not cause issues for the entire model.

Interestingly, MFDFA metrics show very little change over trials, with a low standard error. Moreover, MFDFA<sub>Width-Diff</sub> does not significantly change over trials. This indicates that the difference in multifractal width between MI and Rest is a stable metric with little inter-trial variability. This is congruent with the findings of section 4.6, and suggest that long trial effects do not influence MFDFA<sub>Width-Diff</sub>, which indicates that factors such as fatigue or workload are not important for the metric, and successfully get baselined using the rest condition. According to [Li, Shi, and Li \(2024\)](#), mitigating the effects of cognitive load can improve MI classification performance, and thus far this has not been performed through normal baselining methods. A future study could investigate the effects of such a baseline on classification, specifically related to the stability of classification accuracy over the course of a session.

### 6.7 *Limitations*

A key limitation of this study is the selection of a common maximal scale for all trials, set to 312 samples based on the median signal length. While this standardization facilitates comparison, it can bias results by limiting the detection of long-range correlations and structural patterns in longer signals, and increasing variance in shorter signals due to fewer segments for analysis. This inconsistency can affect the robustness of

the statistical analysis across different trials, sessions, and participants. However, given the large number of trials aggregated, it is likely that these biases are averaged out, mitigating their overall impact on the study's findings. Nonetheless, this study should be repeated with more structured data, where all MI attempts are of equal length.

Another limitation of using MFDFA as a metric for real-time Motor Imagery is that it requires significant computational time, making it challenging to implement in real-time applications. The complexity of the analysis means that it takes longer to compute, which can delay feedback. While MFDFA provides valuable insights into signal properties, its longer processing time may reduce its effectiveness in scenarios requiring immediate response and adaptation.

Lastly, this study only used the ERD metric for comparison against the non-linear MFDFA metrics. While ERD is a valuable measure, there are many other metrics for describing motor imagery. For instance, it would be interesting to compare metrics such as variance, as described by Pfurtscheller and Da Silva (1999). Moreover, the study did not include a comparison with ERS metrics. Including a broader range of metrics could provide a more comprehensive comparison of our current understanding of motor imagery, and how a non-linear metric like multifractal width can be used to enhance the robustness of the MI classifiers.

## 7 CONCLUSION

This study explored the multifractal characteristics of EEG signals during MI, focusing on the complexities and interactions within MI-related signals. Moreover, it provided new insights that could be used to combat BCI inefficiency such as inter trial and subject variability.

This was done by first investigating the general characteristics of multifractality during MI, by investigating aggregates of MFDFA plots (RQ1). These characteristics were then compared to already established (linear) metrics, as well as between two performance groups (RQ2), highlighting the similarities, such as the presence of contra lateralization, mainly in the high performing group. Moreover, this thesis provided a longitudinal perspective, showing the change of MI descriptors over the course of MI training (RQ3).

The main contribution of this thesis is to provide a baseline understanding of what the multifractal characteristics of MI are. Moreover, this thesis has highlighted a few interesting dynamics in multifractality of MI that can be used in combating BCI inefficiency. For example, it became evident that MFDFA<sub>Width-Diff</sub> could possibly serve as a trial-invariant variable, which could allow for a decrease in inter trial variability. Moreover, future work

has been suggested, which suggests new features, such as the range of Hurst exponents, that could reduce inter subject variability.

Nonetheless, this thesis has offered a fresh perspective on the brain dynamics underlying MI, particularly through the lens of MFDFA. These findings contribute to a deeper understanding of neural activity during motor imagery and suggest new directions for improving BCI efficiency, particularly in addressing inter-trial and inter-subject variability. By integrating multifractal analysis with traditional metrics, future research can further refine BCI technology, enhancing its accuracy, reliability, and accessibility for BCI inefficient users.

#### REFERENCES

- Aftanas, L., & Golocheikine, S. (2002). Non-linear dynamic complexity of the human EEG during meditation. , 330(2), 143–146. Retrieved 2024-05-20, from <https://linkinghub.elsevier.com/retrieve/pii/S0304394002007450> doi: 10.1016/S0304-3940(02)00745-0
- Bashashati, A., Fatourechi, M., Ward, R. K., & Birch, G. E. (2007). A survey of signal processing algorithms in brain-computer interfaces based on electrical brain signals. , 4(2), R32–R57. Retrieved 2024-05-17, from <https://iopscience.iop.org/article/10.1088/1741-2560/4/2/R03> doi: 10.1088/1741-2560/4/2/R03
- Bovend'Eerdt, T. J., Dawes, H., Sackley, C., Izadi, H., & Wade, D. T. (2010). An integrated motor imagery program to improve functional task performance in neurorehabilitation: a single-blind randomized controlled trial. *Archives of physical medicine and rehabilitation*, 91(6), 939–946.
- Brodu, N., Lotte, F., & Lécuyer, A. (2012). Exploring two novel features for EEG-based brain-computer interfaces: Multifractal cumulants and predictive complexity. , 79, 87–94. Retrieved 2024-02-26, from <https://www.sciencedirect.com/science/article/pii/S0925231211006291> (Publisher: Elsevier)
- Chatterjee, S., Pratiher, S., & Bose, R. (2017). Multifractal detrended fluctuation analysis based novel feature extraction technique for automated detection of focal and non-focal electroencephalogram signals<? show [aq id= q1]?>. *IET Science, Measurement & Technology*, 11(8), 1014–1021.
- Doyle, L. M., Yarrow, K., & Brown, P. (2005). Lateralization of event-related beta desynchronization in the EEG during pre-cued reaction time tasks. , 116(8), 1879–1888. Retrieved from <https://linkinghub.elsevier.com/retrieve/pii/S1388245705001458> doi: 10.1016/j

- .clinph.2005.03.017
- Gaurav, G., Anand, R. S., & Kumar, V. (2021). EEG based cognitive task classification using multifractal detrended fluctuation analysis. , 15(6), 999–1013. Retrieved 2024-02-12, from <https://link.springer.com/10.1007/s11571-021-09684-z> doi: 10.1007/s11571-021-09684-z
- Geronimo, A., & Simmons, Z. (2020). Telebci: remote user training, monitoring, and communication with an evoked-potential brain-computer interface. *Brain-Computer Interfaces*, 7(3-4), 57–69.
- Gerstner, W. (2011). Hebbian learning and plasticity. *From neuron to cognition via computational neuroscience*, 0–25.
- Gu, G.-F., & Zhou, W.-X. (2006). Detrended fluctuation analysis for fractals and multifractals in higher dimensions. *Physical Review E*, 74(6), 061104.
- Hardstone, R., Poil, S.-S., Schiavone, G., Jansen, R., Nikulin, V. V., Mansvelder, H. D., & Linkenkaer-Hansen, K. (2012). Detrended fluctuation analysis: a scale-free view on neuronal oscillations. *Frontiers in physiology*, 3, 23105.
- Hashimoto, Y., Ushiba, J., Kimura, A., Liu, M., & Tomita, Y. (2010). Change in brain activity through virtual reality-based brain-machine communication in a chronic tetraplegic subject with muscular dystrophy. *BMC neuroscience*, 11, 1–9.
- Huang, G., Zhao, Z., Zhang, S., Hu, Z., Fan, J., Fu, M., ... Dan, G. (2023). Discrepancy between inter-and intra-subject variability in EEG-based motor imagery brain-computer interface: Evidence from multiple perspectives. , 17, 1122661. Retrieved 2024-02-12, from <https://www.frontiersin.org/articles/10.3389/fnins.2023.1122661/full> (Publisher: Frontiers)
- Ihlen, E. A., & Vereijken, B. (2010). Interaction-dominant dynamics in human cognition: Beyond  $1/f$  fluctuation. , 139(3), 436. Retrieved 2024-02-26, from <https://psycnet.apa.org/journals/xge/139/3/436/> (Publisher: American Psychological Association)
- Kantelhardt, J. W., Zschiegner, S. A., Koscielny-Bunde, E., Havlin, S., Bunde, A., & Stanley, H. E. (2002). Multifractal detrended fluctuation analysis of nonstationary time series. *Physica A: Statistical Mechanics and its Applications*, 316(1-4), 87–114.
- Kelty-Stephen, D. G., Lane, E., Bloomfield, L., & Mangalam, M. (2022). Multifractal test for nonlinearity of interactions across scales in time series. , 55(5), 2249–2282. Retrieved 2024-02-11, from <https://link.springer.com/10.3758/s13428-022-01866-9> doi: 10.3758/s13428-022-01866-9
- Kelty-Stephen, D. G., Palatinus, K., Saltzman, E., & Dixon, J. A. (2013). A tutorial on multifractality, cascades, and interactivity for empirical

- time series in ecological science. , 25(1), 1–62. Retrieved 2024-02-11, from <http://www.tandfonline.com/doi/abs/10.1080/10407413.2013.753804> doi: 10.1080/10407413.2013.753804
- Lee, S., Lee, C.-H., Kim, H., & Kim, D.-j. (2020). Lateralization of alpha oscillation under preparation lead to efficiency of motor imagery: Related with performance of classification. In *2020 IEEE international conference on systems, man, and cybernetics (SMC)* (pp. 2502–2505). IEEE. Retrieved from <https://ieeexplore.ieee.org/document/9283439/> doi: 10.1109/SMC42975.2020.9283439
- Li, J., Shi, W., & Li, Y. (2024). An effective classification approach for eeg-based motor imagery tasks combined with attention mechanisms. *Cognitive Neurodynamics*, 1–19.
- Likens, A., & Wiltshire, T. J. (2023). fractalregression: An r package for multiscale regression and fractal analyses.
- Lotze, M., & Halsband, U. (2006). Motor imagery. , 99(4), 386–395. Retrieved from <https://www.sciencedirect.com/science/article/pii/S0928425706000210> (Publisher: Elsevier)
- Lu, Y., & Rodriguez-Larios, J. (2022). Nonlinear eeg signatures of mind wandering during breath focus meditation. *Current Research in Neurobiology*, 3, 100056.
- Nakayashiki, K., Saeki, M., Takata, Y., Hayashi, Y., & Kondo, T. (2014). Modulation of event-related desynchronization during kinematic and kinetic hand movements. , 11(1), 90. Retrieved 2024-02-11, from <https://jneuroengrehab.biomedcentral.com/articles/10.1186/1743-0003-11-90> doi: 10.1186/1743-0003-11-90
- Nam, C. S., Jeon, Y., Kim, Y.-J., Lee, I., & Park, K. (2011). Movement imagery-related lateralization of event-related (de) synchronization (erd/ers): motor-imagery duration effects. *Clinical Neurophysiology*, 122(3), 567–577.
- Neuper, C., Wörtz, M., & Pfurtscheller, G. (2006). ERD/ERS patterns reflecting sensorimotor activation and deactivation. , 159, 211–222. Retrieved 2024-02-11, from <https://www.sciencedirect.com/science/article/pii/S0079612306590144> (Publisher: Elsevier)
- Padfield, N., Zabalza, J., Zhao, H., Masero, V., & Ren, J. (2019). EEG-based brain-computer interfaces using motor-imagery: Techniques and challenges. , 19(6), 1423. Retrieved 2024-02-26, from <https://www.mdpi.com/1424-8220/19/6/1423> (Publisher: MDPI)
- Paul, S., Mazumder, A., Ghosh, P., Tibarewala, D., & Vimalarani, G. (2015). Eeg based emotion recognition system using mfdfa as feature extractor. In *2015 international conference on robotics, automation, control and embedded systems (race)* (pp. 1–5).
- Perquin, M. N., Van Vugt, M. K., Hedge, C., & Bompas, A. (2023). Temporal

- structure in sensorimotor variability: A stable trait, but what for? , 6(3), 400–437. Retrieved 2024-02-12, from <https://link.springer.com/10.1007/s42113-022-00162-1> doi: 10.1007/s42113-022-00162-1
- Pfurtscheller, G. (2000). Spatiotemporal ERD/ERS patterns during voluntary movement and motor imagery. , 53, 196–198. Retrieved 2024, from <https://www.sciencedirect.com/science/article/pii/S1567424X09701576> (Publisher: Elsevier)
- Pfurtscheller, G., & Da Silva, F. L. (1999). Event-related eeg/meg synchronization and desynchronization: basic principles. *Clinical neurophysiology*, 110(11), 1842–1857.
- Prasad, G., Herman, P., Coyle, D., McDonough, S., & Crosbie, J. (2010). Applying a brain-computer interface to support motor imagery practice in people with stroke for upper limb recovery: a feasibility study. , 7(1), 60. Retrieved 2024-02-11, from <https://jneuroengrehab.biomedcentral.com/articles/10.1186/1743-0003-7-60> doi: 10.1186/1743-0003-7-60
- Prinsen, J. (2024). *Master thesis*. Retrieved from <https://github.com/JosPrinsen/MasterThesis.git> (Accessed: 2024-06-24)
- Proteau-Lemieux, M., Knoth, I. S., Agbogba, K., Côté, V., Barlahan Biag, H. M., Thurman, A. J., ... others (2021). Eeg signal complexity is reduced during resting-state in fragile x syndrome. *Frontiers in psychiatry*, 12, 716707.
- Sheahan, H. R., Ingram, J. N., Žalalytė, G. M., & Wolpert, D. M. (2018). Imagery of movements immediately following performance allows learning of motor skills that interfere. , 8(1), 14330. Retrieved 2024-02-26, from <https://www.nature.com/articles/s41598-018-32606-9> (Publisher: Nature Publishing Group UK London)
- Sikdar, D., Roy, R., & Mahadevappa, M. (2018). Epilepsy and seizure characterisation by multifractal analysis of eeg subbands. *Biomedical Signal Processing and Control*, 41, 264–270.
- Solodkin, A., Hlustik, P., Chen, E. E., & Small, S. L. (2004). Fine modulation in network activation during motor execution and motor imagery. *Cerebral cortex*, 14(11), 1246–1255.
- Stieger, J. R., Engel, S., Jiang, H., Cline, C. C., Kreitzer, M. J., & He, B. (2020). Mindfulness improves brain–computer interface performance by increasing control over neural activity in the alpha band. , 31(1), 426–438. Retrieved from <https://doi.org/10.1093/cercor/bhaa234> (\_eprint: <https://academic.oup.com/cercor/article-pdf/31/1/426/34841148/bhaa234.pdf>) doi: 10.1093/cercor/bhaa234
- Stoykov, M. E., Corcos, D. M., & Madhavan, S. (2017). Movement-based priming: clinical applications and neural mechanisms. *Journal of*

- motor behavior*, 49(1), 88–97.
- Tariq, M., Trivailo, P. M., & Simic, M. (2018). Eeg-based bci control schemes for lower-limb assistive-robots. *Frontiers in human neuroscience*, 12, 312.
- Wendt, H., Abry, P., & Jaffard, S. (2007). Bootstrap for empirical multifractal analysis. *IEEE signal processing magazine*, 24(4), 38–48.
- Wriessnegger, S. C., Müller-Putz, G. R., Brunner, C., & Sburlea, A. I. (2020). Inter-and intra-individual variability in brain oscillations during sports motor imagery. , 14, 576241. Retrieved 2024, from <https://www.frontiersin.org/articles/10.3389/fnhum.2020.576241/full> (Publisher: Frontiers Media SA)
- Xu, T. L., De Barbaro, K., Abney, D. H., & Cox, R. F. (2020). Finding structure in time: Visualizing and analyzing behavioral time series. *Frontiers in Psychology*, 11, 521451.
- Zhang, R., Li, F., Zhang, T., Yao, D., & Xu, P. (2020). Subject inefficiency phenomenon of motor imagery brain-computer interface: Influence factors and potential solutions. , 6(3), 224–241. Retrieved 2024-02-26, from <http://journals.sagepub.com/doi/10.26599/BSA.2020.9050021> doi: 10.26599/BSA.2020.9050021

8 APPENDIX

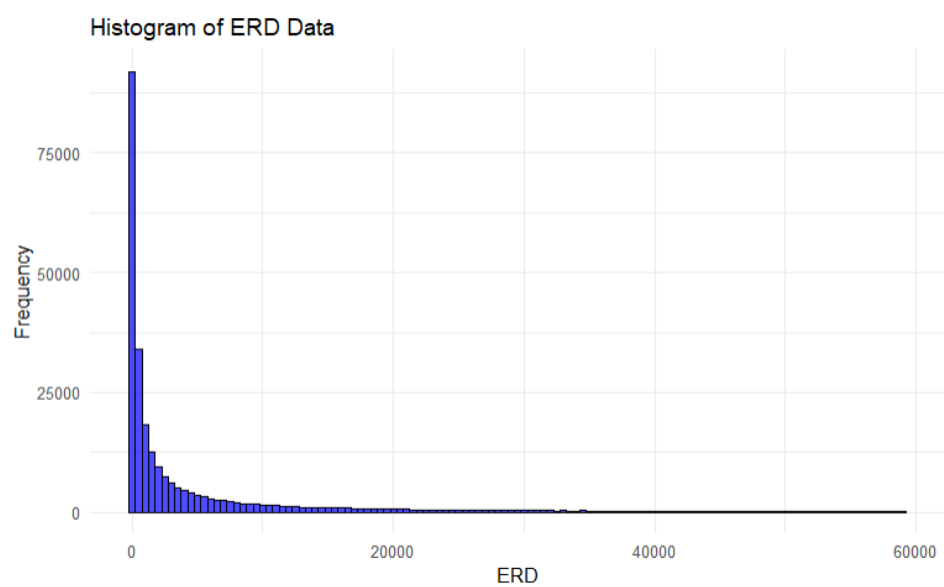


Figure 9: Distribution of ERD values